

UCRHEP-T206

October 1997

Probing New Higgs-Top Interactions at the Tree-Level in a Future e^+e^- Collider ¹

Shaouly Bar-Shalom

Department of Physics, University of California,
Riverside CA 92521, USA.

Abstract

The possibility of observing large signatures of new CP-violating and flavor-changing Higgs-Top couplings in a future e^+e^- collider experiments such as $e^+e^- \rightarrow t\bar{t}h$, $t\bar{t}Z$ and $e^+e^- \rightarrow t\bar{c}\nu_e\bar{\nu}_e$, $t\bar{c}e^+e^-$ is discussed. Such, beyond the Standard Model, couplings can occur already at the tree-level within a class of Two Higgs Doublets Models. Therefore, an extremely interesting feature of those reactions is that the CP-violating and flavor-changing effects are governed by tree-level dynamics. These reactions may therefore serve as unique avenues for searching for new phenomena associated with Two Higgs Doublets Models and, as is shown here, could yield statistically significant signals of new physics. We find that the CP-asymmetries in $e^+e^- \rightarrow t\bar{t}h$, $t\bar{t}Z$ can reach tens of percents, and the flavor changing cross-section of $e^+e^- \rightarrow t\bar{c}\nu_e\bar{\nu}_e$ is typically a few fb's, for light Higgs mass around the electroweak scale.

¹Expanded version of a talk presented at the International Europhysics Conference on High Energy Physics, EPS-HEP97, August 19-26, 1997, Jerusalem, Israel; Based on works done in collaboration with D. Atwood, G. Eilam, A. Soni and J. Wudka.

2. Introductory Remarks And Two Higgs Doublets Models

A future high energy e^+e^- collider running at c.m. energies of 0.5–2 TeV, often referred to as the Next Linear Collider (NLC), is designed, in part, to study in detail the nature of the scalar potential [1]. It may be also very useful for a close examination of the top quark Yukawa couplings to scalar particle(s) which, in turn, may give us a clue about the properties of the scalar particle(s).

In a NLC with a yearly integrated luminosity of the order of 100 fb^{-1} , a detailed study of cross-sections at the level of $\sim \text{few fb's}$ may become feasible. In particular, for top-Higgs systems, the NLC will enable a detailed examination of new phenomena, beyond the Standard Model (SM), associated with new CP-violating and flavor-changing (FC) top Yukawa couplings to scalar particle(s), such as the ones discussed here. Indeed, the top quark, being so heavy, $m_t \sim 175 \text{ GeV}$, is the most sensitive to these new interactions.

In the SM, the scalar potential is economically composed of only one scalar doublet. Even a mild extension of the SM with an additional scalar doublet [2], can give rise to rich new phenomena beyond the SM associated with top-Higgs systems, e.g., tree-level CP-violation [3, 4, 5] and tree-level flavor-changing-scalar (FCS) transitions [6, 7, 8], in interaction of neutral scalars with the top quark.

Here we present three distinct reactions which are very powerful probes of the tth and $t\bar{c}h$ Yukawa couplings. The first two reactions, $e^+e^- \rightarrow t\bar{t}h$ and $e^+e^- \rightarrow t\bar{t}Z$ [3, 4], exhibit large CP-violating asymmetries, at the order of tens of percent, already at *tree-level*. The third is *tree-level* $t\bar{c}$ production through the W^+W^- fusion process, $e^+e^- \rightarrow W^+W^- \nu_e \bar{\nu}_e \rightarrow t\bar{c} \nu_e \bar{\nu}_e$ [6], which appears to be extremely sensitive to a $t\bar{c}h$ FCS interaction.

In the presence of two Higgs doublets the most general Yukawa lagrangian can be written as:

$$\mathcal{L}_Y = U_{ij}^1 \bar{q}_{i,L} \tilde{\phi}_1 u_{j,R} + D_{ij}^1 \bar{q}_{i,L} \phi_1 d_{j,R} + U_{ij}^2 \bar{q}_{i,L} \tilde{\phi}_2 u_{j,R} + D_{ij}^2 \bar{q}_{i,L} \phi_2 d_{j,R} + \text{h.c.} , \quad (1)$$

where ϕ_i for $i = 1, 2$ are the two scalar doublets and U_{ij}^k, D_{ij}^k , for $k = 1, 2$, are the Yukawa couplings matrices which are in general non-diagonal. Depending on

the assumptions made, one can then obtain different versions of a Two Higgs Doublet Model (2HDM). In particular, if one imposes the discrete symmetries $\phi_1; \phi_2 \rightarrow -\phi_1; \phi_2$ and $d_{i,R}; u_{i,R} \rightarrow -d_{i,R}; -u_{i,R}$ or $-d_{i,R}; u_{i,R}$ one arrives at the so called Model I or Model II, respectively, depending on whether the -1/3 and 2/3 charged quarks are coupled to the same or to different scalar doublets. If, in addition, these discrete symmetries are softly violated by a mass-dimension-two term in the Higgs potential, then the real and imaginary parts of the Higgs doublets mix, giving rise to CP-violating scalar-pseudoscalar mixed couplings of a neutral Higgs to fermions already at the tree-level [9]. On the other hand, if one does not impose the above discrete symmetries, one arrives at a most general version of the 2HDM, often called Model III, in which both FCS transitions and CP-nonconserving interactions between the neutral Higgs particles and fermions are present at tree-level (for a recent short review see e.g., [10]). The scalar spectrum of any of the above 2HDM's consists of three neutral Higgs and two charged Higgs particles which are not relevant for the present discussion. For reasons discussed in the following sections, for both the CP-violating effects in $e^+e^- \rightarrow t\bar{t}h, t\bar{t}Z$ and the FC effects in $e^+e^- \rightarrow t\bar{c}\nu_e\bar{\nu}_e$, only two out of the three neutral Higgs of the 2HDM's (i.e., Models II and III) are relevant. We denote these two neutral Higgs particles by h and H corresponding to the lighter and heavier Higgs-boson, respectively. In some instances we denote a neutral Higgs by \mathcal{H} , then $\mathcal{H} = h$ or H is to be understood.

The $\mathcal{H}t\bar{t}$ interaction lagrangian piece of a general 2HDM can be written as:

$$\mathcal{L}_{\mathcal{H}tt} = -\frac{g_W}{\sqrt{2}} \frac{m_t}{m_W} \mathcal{H} \bar{t} \left(a_t^{\mathcal{H}} + i b_t^{\mathcal{H}} \gamma_5 \right) t, \quad (2)$$

where in Model II used here:

$$a_t^h; a_t^H = \frac{R_{11}}{\sin \beta}; \frac{R_{12}}{\sin \beta}, \quad b_t^h; b_t^H = \frac{R_{31}}{\tan \beta}; \frac{R_{32}}{\tan \beta}. \quad (3)$$

$\tan \beta \equiv v_u/v_d$ and $v_u(v_d)$ is the vacuum-expectation-value (VEV) responsible for giving mass to the up(down) quark. R is the neutral Higgs mixing matrix which can be parameterized by three Euler angles $\alpha_{1,2,3}$ [9]. Note that in the SM the only couplings in Eqs. 2 and 3, of the one neutral Higgs present, are $a_t^h = 1/\sqrt{2}, b_t^h = 0$ and there is no phase in the $ht\bar{t}$ interaction lagrangian.

In Model III with the Cheng-Sher Ansatz (CSA) [11], the couplings of the neutral scalars to fermions are given by $\xi_{ij}^{U,D} = g_W \left(\sqrt{m_i m_j} / m_W \right) \lambda_{ij}$ and the $t\bar{c}h$ interaction Lagrangian can then be written as:

$$\mathcal{L}_{\mathcal{H}tc} = -\frac{g_W}{\sqrt{2}} \frac{\sqrt{m_t m_c}}{m_W} f^{\mathcal{H}} \mathcal{H} \bar{t} (\lambda_R + i\lambda_I \gamma_5) c, \quad (4)$$

where for simplicity we choose $\lambda_{tc} = \lambda_{ct} = \lambda$.² We furthermore break λ into its real and imaginary parts, $\lambda = \lambda_R + i\lambda_I$. Also, in the framework of Model III described in [10], where only one Higgs doublet acquires a VEV, one has:

$$f^h; f^H = \cos \tilde{\alpha}; \sin \tilde{\alpha}, \quad (5)$$

and the mixing angle $\tilde{\alpha}$ is determined by the Higgs potential.

We will also need the $\mathcal{H}VV$ couplings ($V = W^+, W^-$ or Z), which can be written in general as:

$$\mathcal{L}_{\mathcal{H}VV} = g_W m_W C_V c^{\mathcal{H}} \mathcal{H} g_{\mu\nu} V^\mu V^\nu, \quad (6)$$

where $C_W; C_Z \equiv 1; m_Z^2/m_W^2$. For Models II and III we have:

$$\text{Model II} \quad : \quad c^h; c^H = R_{11} \sin \beta + R_{21} \cos \beta; R_{12} \sin \beta + R_{22} \cos \beta, \quad (7)$$

$$\text{Model III} \quad : \quad c^h; c^H \equiv -\sin \tilde{\alpha}; \cos \tilde{\alpha}. \quad (8)$$

Note that in the SM the only VVh coupling of the one neutral Higgs present is $c^h = 1$.

²Existing experimental information does not provide any useful constraints on λ_{tc} ; in particular, we may well have $\lambda_{tc} \sim \mathcal{O}(1)$ [10].

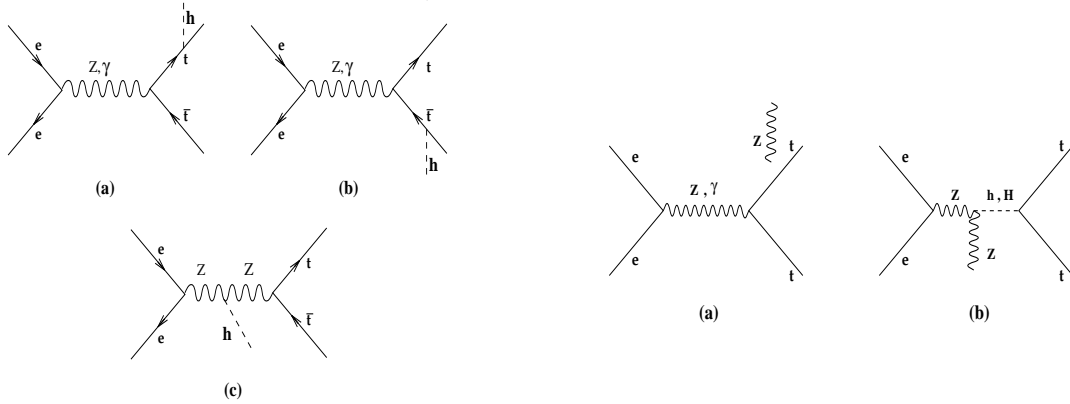


Figure 1: Tree-level Feynman diagrams contributing to $e^+e^- \rightarrow t\bar{t}h$ (left hand side) and $e^+e^- \rightarrow t\bar{t}Z$ (right hand side) in the unitary gauge, in a two Higgs doublet model. For $e^+e^- \rightarrow t\bar{t}Z$, Diagram (a) on the right hand side represents 8 diagrams in which either Z or γ are exchanged in the s-channel and the outgoing Z is emitted from e^+, e^-, t or \bar{t} .

3. $e^+e^- \rightarrow t\bar{t}h, t\bar{t}Z$; Cases of Tree-Level CP-Violation³

The reactions:

$$e^+(p_+) + e^-(p_-) \rightarrow t(p_t) + \bar{t}(p_{\bar{t}}) + h(p_h) , \quad (9)$$

$$e^+(p_+) + e^-(p_-) \rightarrow t(p_t) + \bar{t}(p_{\bar{t}}) + Z(p_Z) , \quad (10)$$

exhibits large CP violation asymmetries in a 2HDM. A novel feature of these reactions is that the effect arises at tree graph level. Basically, for the $t\bar{t}h(t\bar{t}Z)$ final states, Higgs(Z) emission off the t, \bar{t} interferes with the Higgs(Z) emission off the s-channel Z -boson (see Fig. 1) [3, 4]. We find that the processes $e^+e^- \rightarrow t\bar{t}h$ and $e^+e^- \rightarrow t\bar{t}Z$ provide two independent, but analogous, promising venues to search for signatures of the same CP-odd phase, residing in the top-neutral Higgs coupling, if the value of $\tan\beta$ (the ratio between the two VEV's in a 2HDM) is in the vicinity of 1. In particular, they serve as good examples for large CP-violating effects that could emanate from t systems due to the large mass of the top quark and, thus, they might unveil the role of a neutral Higgs particle in CP-violation.

³This section will appear in a review paper: "CP-Violation in Top Physics", by D. Atwood, S. Bar-Shalom, G. Eilam and A. Soni, to be submitted to Physics Reports.

Although these reactions are not meant (necessarily) to lead to the discovery of a neutral Higgs, they will, no doubt, be scrutinized in the NLC since they stand out as very interesting channels by themselves. In particular, they could perhaps provide a unique opportunity to observe the top-Higgs Yukawa couplings directly [12, 13, 14]. In [12, 13], using a very interesting generalization of the optimal observables technique used here, Gunion *et al.* have extended our work on CP-violation in $e^+e^- \rightarrow t\bar{t}h$ described below, to include a detailed cross-section analysis such that all Higgs Yukawa couplings combinations are extracted. A detailed cross-section analysis of the reaction $e^+e^- \rightarrow t\bar{t}Z$ was performed in the SM by Hagiwara *et al.* [14]. There, it was found that the Higgs exchange contribution of diagram (b) on the right hand side of Fig. 1 will be almost invisible in a TeV e^+e^- collider for neutral Higgs masses in the range $m_h < 2m_t$. On the contrary, we will show here that if the scalar sector is doubled, then the lightest neutral Higgs may reveal itself through CP-violating interactions with the top quark even if $m_h < 2m_t$.

In the unitary gauge the reactions in Eqs. 9 and 10 can proceed via the Feynman diagrams depicted in Fig. 1. We see that for $e^+e^- \rightarrow t\bar{t}Z$, diagram (b) on the right hand side of Fig. 1, in which Z and \mathcal{H} are produced ($\mathcal{H} = h$ or H is either a real or virtual particle, i.e. $m_{\mathcal{H}} > 2m_t$ or $m_{\mathcal{H}} < 2m_t$, respectively) followed by $\mathcal{H} \rightarrow t\bar{t}$, is the only place where new CP-nonconserving dynamics from the Higgs sector can arise, being proportional to the CP-odd phase in the $\mathcal{H}t\bar{t}$ vertex. As mentioned above, in both the $t\bar{t}h$ and the $t\bar{t}Z$ final state cases, CP-violation arises due to interference of the diagrams where the Higgs is coupled to a Z-boson with the diagrams where the Higgs or Z is radiated off the t or \bar{t} . We note that in the $t\bar{t}Z$ case there is no CP-violating contribution coming from the interference between the diagrams with the $ZZ\mathcal{H}$ coupling and the diagrams where the Z-boson is emitted from the incoming electron or positron lines.

The relevant pieces of the interaction Lagrangian involve the $\mathcal{H}t\bar{t}$ and the $\mathcal{H}ZZ$ couplings and is given in Eqs. 2 and 6, respectively. As usual the couplings $a_t^{h,H}$, $b_t^{h,H}$ and $c^{h,H}$ in Eqs. 3 and 7, respectively, are functions of $\tan\beta \equiv v_2/v_1$ (the ratio of the two VEVs) and of the three mixing angles $\alpha_1, \alpha_2, \alpha_3$ which characterize the Higgs mass matrix. As was mentioned in the previous section, only two (denoted

here by h and H) out of the three neutral Higgs are relevant for the CP-violating effect studied here. The reason is that only two out of the three neutral Higgs particles in the theory can simultaneously have a coupling to vector bosons and a pseudoscalar coupling to fermions. We have denoted their couplings by a_t^h, b_t^h, c^h and a_t^H, b_t^H, c^H , corresponding to the light, h , and heavy, H , neutral Higgs, respectively. This implies the existence of a “GIM-like” cancellation, namely, when both h and H contribute to CP-violation, then all CP-nonconserving effects, being proportional to $b_t^h c^h + b_t^H c^H$, must vanish when the two Higgs states h and H are degenerate. In the following we set the mass of the heavy Higgs, H , to be $m_H = 750$ GeV or 1 TeV.

In the process $e^+e^- \rightarrow t\bar{t}h$, a Higgs particle is produced in the final state, therefore, the heavy Higgs-boson, H , is not important and this “GIM-like” mechanism is irrelevant. Note that there is an additional diagram contributing to $e^+e^- \rightarrow t\bar{t}h$, which involve the ZhH coupling and is not shown in Fig. 1. This diagram is, however, negligible for the large m_H values used here. In contrast, in the process $e^+e^- \rightarrow t\bar{t}Z$, the Higgs is exchanged as a virtual or a real particle and the effect of H is, although small compared to h , important in order to restore the “GIM-like” cancellation discussed above.

For both the $t\bar{t}h$ and $t\bar{t}Z$ final states processes, we denote the tree-level polarized differential-cross-section (DCS) by $\Sigma_{(j)f}$, where $f = t\bar{t}h$ or $f = t\bar{t}Z$ corresponding to the $t\bar{t}h$ or $t\bar{t}Z$ final states, respectively, and $j = 1(-1)$ for left(right) polarized incoming electron beam. $\Sigma_{(j)f}$ can be subdivided into its CP-even ($\Sigma_{+(j)f}$) and CP-odd ($\Sigma_{-(j)f}$) parts:

$$\Sigma_{(j)f} = \Sigma_{+(j)f} + \Sigma_{-(j)f} . \quad (11)$$

The CP-even and CP-odd DCS’s can be further broken to different terms which correspond to the various Higgs coupling combinations and which transform as n under T_N . For both final states, $f = t\bar{t}h$ and $f = t\bar{t}Z$, we have:

$$\Sigma_{+(j)f} = \sum_i g_{+f}^{i(n)} F_{+(j)f}^{i(n)} , \quad \text{CP even} , \quad (12)$$

$$\Sigma_{-(j)f} = \sum_i g_{-f}^{i(n)} F_{-(j)f}^{i(n)} , \quad \text{CP odd} , \quad (13)$$

where $g_{+f}^{i(n)}, g_{-f}^{i(n)}$, $n = +$ or $-$, are different combinations of the Higgs couplings $a_t^{\mathcal{H}}, b_t^{\mathcal{H}}, c^{\mathcal{H}}$ and $F_{+(j)f}^{i(n)}, F_{-(j)f}^{i(n)}$, again with $n = +$ or $-$, are kinematical functions of phase space which transform like n under T_N .

Let us first write the Higgs coupling combinations for the CP-even part. In the case of $e^+e^- \rightarrow t\bar{t}h$, neglecting the imaginary part in the s-channel Z propagator, we have four relevant coupling combinations [3, 12]:

$$g_{+tth}^{1(+)} = (a_t^h)^2, \quad g_{+tth}^{2(+)} = (b_t^h)^2, \quad g_{+tth}^{3(+)} = (c^h)^2, \quad g_{+tth}^{4(+)} = a_t^h c^h. \quad (14)$$

In the case of $e^+e^- \rightarrow t\bar{t}Z$, apart from the SM DCS, which corresponds to interference terms among the four SM diagrams represented by diagram (a) on the right hand side of Fig. 1, and keeping terms proportional to both the real and imaginary parts of the Higgs propagator, $\Pi_{\mathcal{H}}$, we get [4]:

$$g_{+ttZ}^{1(+)} = (a_t^{\mathcal{H}} c^{\mathcal{H}}) \text{Re}(\Pi_{\mathcal{H}}), \quad g_{+ttZ}^{2(-)} = (a_t^{\mathcal{H}} c^{\mathcal{H}}) \text{Im}(\Pi_{\mathcal{H}}), \quad (15)$$

$$g_{+ttZ}^{3(+)} = (a_t^{\mathcal{H}} c^{\mathcal{H}})^2 \text{Re}(\Pi_{\mathcal{H}}), \quad g_{+ttZ}^{4(+)} = (a_t^{\mathcal{H}} c^{\mathcal{H}})^2 \text{Im}(\Pi_{\mathcal{H}}), \quad (16)$$

$$g_{+ttZ}^{5(+)} = (b_t^{\mathcal{H}} c^{\mathcal{H}})^2 \text{Re}(\Pi_{\mathcal{H}}), \quad g_{+ttZ}^{6(+)} = (b_t^{\mathcal{H}} c^{\mathcal{H}})^2 \text{Im}(\Pi_{\mathcal{H}}), \quad (17)$$

where:

$$\Pi_{\mathcal{H}} \equiv \left(s + m_Z^2 - m_{\mathcal{H}}^2 - 2p \cdot p_Z + im_{\mathcal{H}} \Gamma_{\mathcal{H}} \right)^{-1}. \quad (18)$$

$p \equiv p_- + p_+$ and $\Gamma_{\mathcal{H}}$ is the width of $\mathcal{H} = h$ or H .

For the CP-odd parts one gets:

$$g_{-tth}^{1(-)} = b_t^h c^h, \quad (19)$$

$$g_{-ttZ}^{1(-)} = b_t^{\mathcal{H}} c^{\mathcal{H}} \text{Re}(\Pi_{\mathcal{H}}), \quad g_{-ttZ}^{2(+)} = b_t^{\mathcal{H}} c^{\mathcal{H}} \text{Im}(\Pi_{\mathcal{H}}). \quad (20)$$

The CP-even pieces, $\Sigma_{+(j)f}$, yield the corresponding cross-sections (recall that $f = t\bar{t}h$ or $t\bar{t}Z$):

$$\sigma_{(j)f} = \int \Sigma_{+(j)f}(\Phi) d\Phi, \quad (21)$$

where Φ stands for the phase-space variables. In Fig. 2a and 2b we plot the unpolarized cross-sections, σ_{tth} and σ_{ttZ} as a function of m_h and \sqrt{s} , for Model II, with $m_H = 750$ GeV and the set of values $\{\alpha_1, \alpha_2, \alpha_3\} = \{\pi/2, \pi/4, 0\}$ which we denote as set II. Set II is also adopted later when discussing the CP-violating effect.

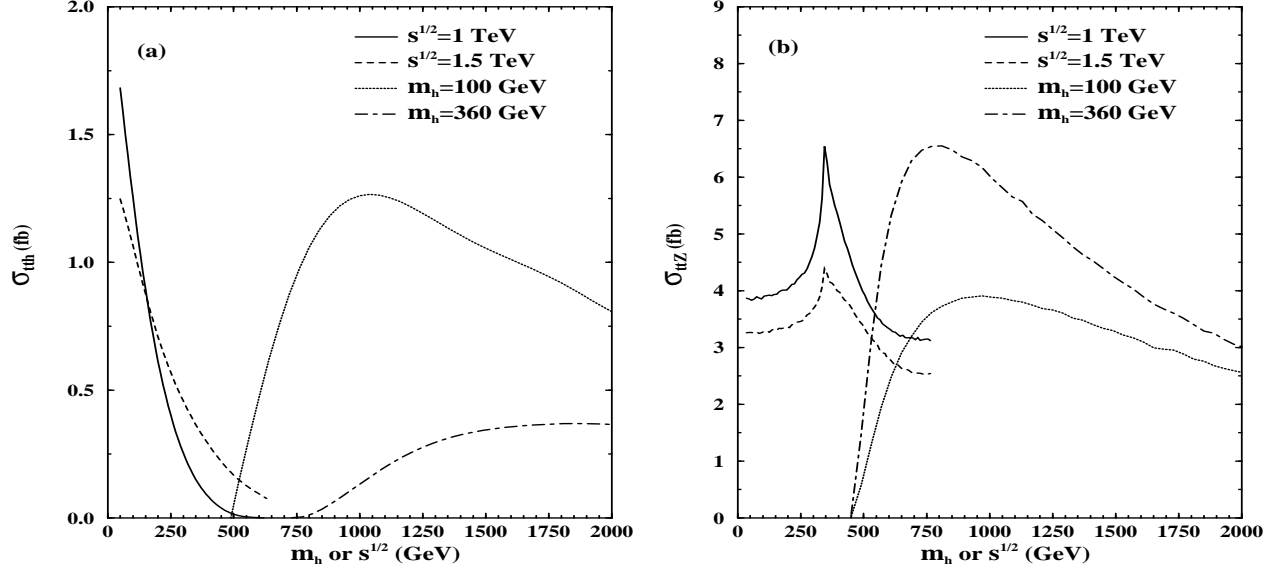


Figure 2: The cross sections (in fb) for: (a) the reaction $e^+e^- \rightarrow t\bar{t}h$ with $\tan\beta = 0.5$ and (b) the reaction $e^+e^- \rightarrow t\bar{t}Z$ with $\tan\beta = 0.3$, assuming unpolarized electron and positron beams, for Model II with set II and as a function of m_h (solid and dashed lines) and \sqrt{s} (dotted and dotted-dashed lines). Set II means $\{\alpha_1, \alpha_2, \alpha_3\} \equiv \{\pi/2, \pi/4, 0\}$.

Furthermore, for the $t\bar{t}h$ final state we choose $\tan\beta = 0.5$ while for $t\bar{t}Z$ we choose $\tan\beta = 0.3$. Afterwards, we will discuss the dependence of the CP-violating effect on $\tan\beta$ in the $t\bar{t}h$ and $t\bar{t}Z$ cases. One can observe the dissimilarities in the two cross-sections $\sigma_{t\bar{t}h}$ and $\sigma_{t\bar{t}Z}$: while $\sigma_{t\bar{t}h}$ is at most ~ 1.5 fb, $\sigma_{t\bar{t}Z}$ can reach ~ 7 fb at around $\sqrt{s} \approx 750$ GeV and $m_h \gtrsim 2m_t$. $\sigma_{t\bar{t}h}$ drops with m_h while $\sigma_{t\bar{t}Z}$ grows in the range $m_h \lesssim 2m_t$. $\sigma_{t\bar{t}Z}$ peaks at around $m_h \gtrsim 2m_t$ and drops as m_h grows further. Moreover, $\sigma_{t\bar{t}h}$ peaks at around $\sqrt{s} \approx 1(1.5)$ TeV for $m_h = 100(360)$ GeV, while $\sigma_{t\bar{t}Z}$ peaks at around $\sqrt{s} \approx 750$ GeV for both $m_h = 100$ and 360 GeV. As we will see later, these different features of the two cross-sections are, in part, the cause for the different behavior of the CP-asymmetries discussed below.

Let us now concentrate on the CP-odd T_N -odd effects in $e^+e^- \rightarrow t\bar{t}h; t\bar{t}Z$, ema-

nating from the T_N -odd pieces in $\Sigma_{-(j)tt\bar{h}}; \Sigma_{-(j)ttZ}$. From Eqs. 19 and 20 it is clear that the CP-violating pieces $\Sigma_{-(j)tt\bar{h}}; \Sigma_{-(j)ttZ}$ have to be proportional to $b_t^h c^h$ (in the ttZ case there is an additional similar piece corresponding to the heavy Higgs H). The corresponding CP-odd kinematic functions, $F_{-(j)tt\bar{h}}^{1(-)}; F_{-(j)ttZ}^{1(-)}$, being T_N -odd, are pure tree-level quantities and are proportional to the only non vanishing Levi-Civita tensor present, $\epsilon(p_-, p_+, p_t, p_{\bar{t}})$, when the spins of the top are disregarded. The explicit expressions for $F_{-(j)f}^{1(-)}$ are:

$$F_{-(j)tt\bar{h}}^{1(-)} = -\frac{1}{\sqrt{2}} \left(\frac{g_W^3}{c_W^3} \right)^2 \frac{m_t^2}{m_Z^2} \Pi_{Zh} \Pi_Z T_t^3 c_j^Z \epsilon(p_-, p_+, p_t, p_{\bar{t}}) \times \\ \left\{ j(\Pi_t^h + \Pi_{\bar{t}}^h) \left[(s - s_t - m_h^2)(3w_j^- - w_j^+) + m_Z^2(w_j^- - w_j^+) \right] + \right. \\ \left. T_t^3 c_j^Z \Pi_Z (\Pi_t^h - \Pi_{\bar{t}}^h) f \right\} , \quad (22)$$

$$F_{-(j)ttZ}^{1(-)} = -\sqrt{2} \left(\frac{2g_W^3}{c_W^3} \right)^2 \frac{m_t^2}{m_Z^2} \Pi_Z T_t^3 c_j^Z \epsilon(p_-, p_+, p_t, p_{\bar{t}}) \times \\ \left\{ j(\Pi_t^Z + \Pi_{\bar{t}}^Z) \left[m_Z^2 w_j^- + (s_t - s) w_j^+ \right] + \right. \\ \left. T_t^3 c_j^Z \Pi_Z (\Pi_t^Z - \Pi_{\bar{t}}^Z) f \right\} , \quad (23)$$

where $s \equiv 2p_- \cdot p_+$ is the c.m. energy of the colliding electrons, $s_t \equiv (p_t + p_{\bar{t}})^2$ and $f \equiv (p_- - p_+) \cdot (p_t + p_{\bar{t}})$. Also:

$$\Pi_{t(\bar{t})}^h \equiv (2p_{t(\bar{t})} \cdot p_h + m_h^2)^{-1} , \quad \Pi_{t(\bar{t})}^Z \equiv (2p_{t(\bar{t})} \cdot p_Z + m_Z^2)^{-1} , \quad (24)$$

$$\Pi_Z \equiv (s - m_Z^2)^{-1} , \quad \Pi_\gamma \equiv s^{-1} , \quad \Pi_{Zh} \equiv ((p - p_h)^2 - m_Z^2)^{-1} . \quad (25)$$

Furthermore:

$$w_j^\pm \equiv \left(s_W^2 Q_t - \frac{1}{2} T_t^3 \right) c_j^Z \Pi_Z \pm Q_t s_W^2 c_W^2 \Pi_\gamma , \quad (26)$$

where $s_W(\cos)$ is the sin(cos) of the weak mixing angle θ_W , Q_f and T_f^3 are the charge and z -component of the weak isospin of a fermion, respectively. $c_{-1}^Z = 1/2 - s_W^2$, $c_1^Z = -s_W^2$ (recall that $j = -1(1)$ for a left(right) handed electron).

Since at tree level there cannot be any absorptive phases, only T_N -odd, CP asymmetries are expected to occur in $\Sigma_{-(j)f}$. Note that in the ttZ case there is a CP-odd T_N -even piece, $b_t^{\mathcal{H}} c^{\mathcal{H}} \text{Im}(\Pi_{\mathcal{H}}) \times F_{-(j)ttZ}^{2(+)}$ (see Eq. 20), in the DCS. However,

being proportional to the absorptive part coming from the Higgs propagator, it is not a pure tree-level quantity.

Simple examples of observables that can trace the tree-level CP-effect in $e^+e^- \rightarrow t\bar{t}h; t\bar{t}Z$ are:

$$O = \frac{\vec{p}_- \cdot (\vec{p}_t \times \vec{p}_{\bar{t}})}{s^{3/2}} \quad , \quad O_{\text{opt}}(t\bar{t}h; t\bar{t}Z) = \frac{\Sigma_{-(j)t\bar{t}h}; \Sigma_{-(j)t\bar{t}Z} (T_N \text{ odd part only})}{\Sigma_{+(j)t\bar{t}h}; \Sigma_{+(j)t\bar{t}Z}} \quad . \quad (27)$$

$O_{\text{opt}}(t\bar{t}h; t\bar{t}Z)$ are optimal observables in the sense that the statistical error, in the measured asymmetry, is minimized [15]. As mentioned before, since the final state consists of three particles, using only the available momenta, there is a unique antisymmetrical tensor that can be formed. Thus, both observables are proportional to $\epsilon(p_-, p_+, p_t, p_{\bar{t}})$ and $O_{\text{opt}}(t\bar{t}h; t\bar{t}Z)$ are related to O through a multiplication by a CP-even function. In the following we focus only on the CP-odd effects coming from the optimal observables. However, we remark that the results for the simple observable O exhibit the same behavior, though slightly smaller than those for O_{opt} . The theoretical statistical significance, N_{SD} , in which an asymmetry can be measured in an ideal experiment is given by $N_{SD} = A\sqrt{L}\sqrt{\sigma}$ ($\sigma = \sigma_{t\bar{t}h}; \sigma_{t\bar{t}Z}$ for the $t\bar{t}h; t\bar{t}Z$ final states), where for the observables O and O_{opt} , the CP-odd quantity A , defined above, is:

$$A_O \approx \langle O \rangle / \sqrt{\langle O^2 \rangle} \quad , \quad A_{\text{opt}} \approx \sqrt{\langle O_{\text{opt}}^2 \rangle} \quad . \quad (28)$$

Also, L is the effective luminosity for fully reconstructed $t\bar{t}h$ or $t\bar{t}Z$ events. In particular, we take $L = \epsilon\mathcal{L}$, where \mathcal{L} is the total yearly integrated luminosity and ϵ is the overall efficiency for reconstruction of the $t\bar{t}h$ or $t\bar{t}Z$ final states.

For numerical results we have used set II defined above for the angles $\alpha_{1,2,3}$, i.e. $\{\alpha_1, \alpha_2, \alpha_3\} = \{\pi/2, \pi/4, 0\}$ (recall that for the $t\bar{t}h$ final state we choose $\tan\beta = 0.5$ while for the $t\bar{t}Z$ final state we choose $\tan\beta = 0.3$). Figs. 3a and 3b show the expected asymmetry and statistical significance in the unpolarized case, corresponding to O_{opt} in Model II for the $t\bar{t}h$ and $t\bar{t}Z$ final states, respectively. The asymmetry is plotted as a function of the mass of the light Higgs (m_h) where again, $m_H = 750$ GeV in the $t\bar{t}Z$ case. We plot N_{SD}/\sqrt{L} , thus scaling out the luminosity factor from the theoretical prediction (as a reference value, we note that for $L = 100 \text{ fb}^{-1}$, $N_{SD}/\sqrt{L} = 0.1$ will correspond to a one-sigma effect). We remark that set II cor-

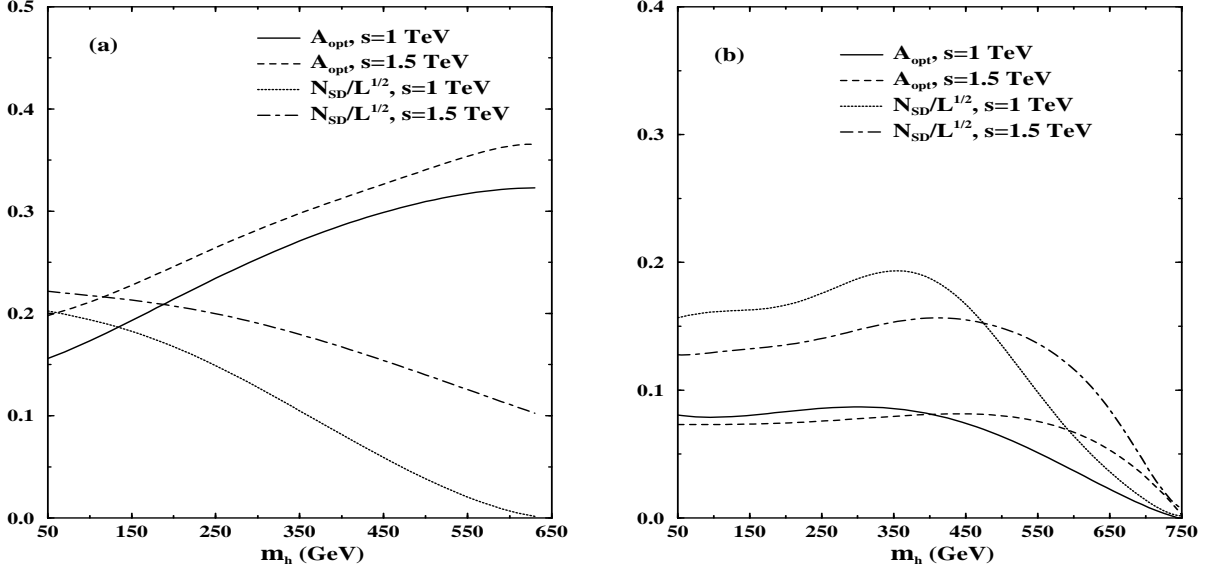


Figure 3: The asymmetry, A_{opt} , and scaled statistical significance, N_{SD}/\sqrt{L} , for the optimal observable O_{opt} for: (a) the reaction $e^+e^- \rightarrow t\bar{t}h$ with $\tan\beta = 0.5$ and (b) the reaction $e^+e^- \rightarrow t\bar{t}Z$ with $\tan\beta = 0.3$, as a function of the light Higgs mass m_h , for $\sqrt{s} = 1$ TeV and 1.5 TeV. All graphs are with set II of the parameters, as in Fig. 2.

responds to the largest CP-effect, though not unique. In the $t\bar{t}h$ case $\tan\beta = 0.5$ is favored, however, the effect mildly depends on $\tan\beta$ in the range $0.3 \lesssim \tan\beta \lesssim 1$ (see also [3]). In the $t\bar{t}Z$ case, the effect is practically insensitive to α_3 and is roughly proportional to $1/\tan\beta$, it therefore drops as $\tan\beta$ is increased. Nonetheless, we find that $N_{SD}/\sqrt{L} > 0.1$, even in the unpolarized case for $\tan\beta \lesssim 0.6$ (see also [4]).

From Fig. 3a we see that, in the $t\bar{t}h$ case, as m_h grows the asymmetry increases while the statistical significance drops, in part because of the decrease in the cross-section. We can see that the asymmetry can become extremely large and it ranges from $\sim 15\%$, for a Higgs mass below 100 GeV, to $\sim 35\%$ for $m_h \sim 600$ GeV. Evidently, the CP-effect is more significant for smaller masses of h , whereas A_{opt} is smaller. In contrast, from Fig. 3b we see that, in the $t\bar{t}Z$ case, A_{opt} stays roughly fixed at around 7 – 8%, for $m_h \lesssim 2m_t$, and then drops till it totally vanishes at

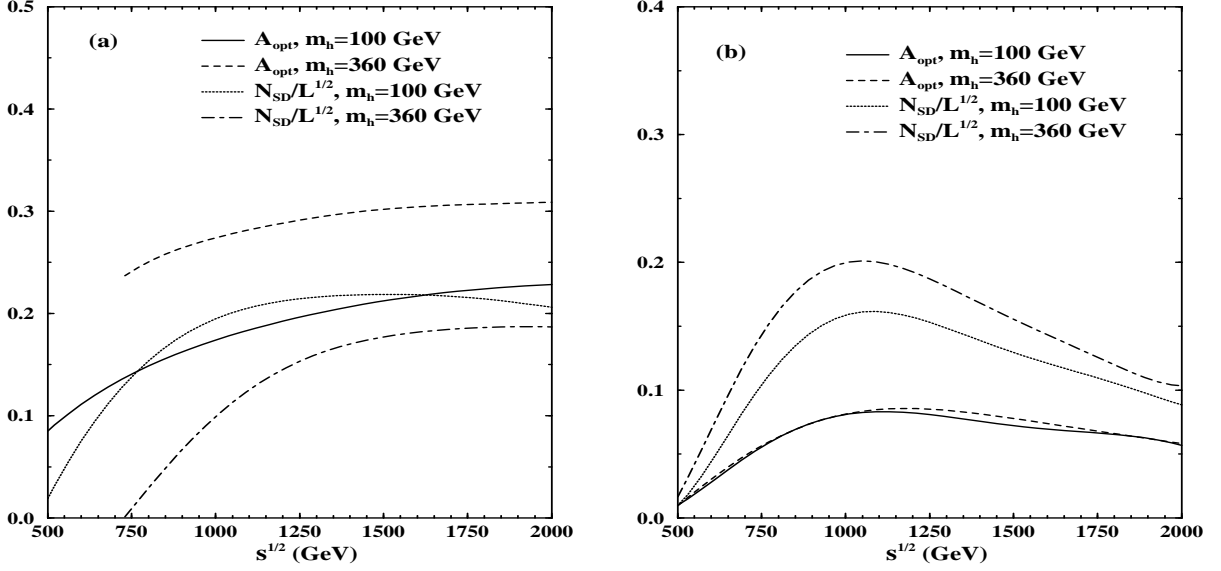


Figure 4: The asymmetry, A_{opt} , and scaled statistical significance, N_{SD}/\sqrt{L} , for the optimal observable O_{opt} for: (a) the reaction $e^+e^- \rightarrow t\bar{t}h$ with $\tan\beta = 0.5$ and (b) the reaction $e^+e^- \rightarrow t\bar{t}Z$ with $\tan\beta = 0.3$, as a function of the c.m. energy \sqrt{s} , for $m_h = 100$ GeV and $m_h = 360$ GeV. All graphs are with set II of the parameters, as in Fig. 2.

$m_h = m_H = 750$ GeV, in which case the “GIM-like” mechanism discussed before applies. The scaled statistical significance N_{SD}/\sqrt{L} behaves roughly as A_{opt} . That is, $N_{SD}/\sqrt{L} \approx 0.12 - 0.2$ in the mass range $50 \text{ GeV} \lesssim m_h \lesssim 350 \text{ GeV}$, for both $\sqrt{s} = 1$ and 1.5 TeV.

Figs. 4a and 4b show the dependence of A_{opt} and N_{SD}/\sqrt{L} on the c.m. energy, \sqrt{s} , for the $t\bar{t}h$ and $t\bar{t}Z$ cases, respectively. We see that, in the case of $t\bar{t}h$, the CP effect peaks at $\sqrt{s} \approx 1.1(1.5)$ TeV for $m_h = 100(360)$ GeV and stays roughly the same as \sqrt{s} is further increased to 2 TeV. In the case of $t\bar{t}Z$, the statistical significance is maximal at around $\sqrt{s} \approx 1$ TeV and then decreases as \sqrt{s} grows, for both $m_h = 100$ and 360 GeV. Contrary to the $t\bar{t}h$ case, where a light h is favored, in the $t\bar{t}Z$ case, the effect is best for $m_h \gtrsim 2m_t$. In that range, on-shell Z and h

are produced followed by the h decay $h \rightarrow t\bar{t}$, thus, the Higgs exchange diagram becomes more dominant.

In Tables 1 and 2 we present N_{SD} for O_{opt} , for the tth and ttZ cases, respectively, in Model II with set II, and we also compare the effect of beam polarization with the unpolarized case. As before, we take $\tan\beta = 0.5$ and $\tan\beta = 0.3$ for the tth and ttZ cases, respectively, where for the ttZ case we also present numbers for both $m_H = 750$ GeV (shown in the parentheses) and $m_H = 1$ TeV, to demonstrate the sensitivity of the CP-effect to the mass of the heavy Higgs. For illustrative purposes, we choose $m_h = 100, 160$ and 360 GeV and show the numbers for $\sqrt{s} = 1$ TeV with $\mathcal{L} = 200$ [fb] $^{-1}$ and for $\sqrt{s} = 1.5$ TeV with $\mathcal{L} = 500$ [fb] $^{-1}$ (see [1]). In both cases we take $\epsilon = 0.5$ assuming that there is no loss of luminosity when the electrons are polarized (if the efficiency for $t\bar{t}h$ and/or ttZ reconstruction is $\epsilon = 0.25$, then our numbers would correspondingly require 2 years of running).

Evidently, for both reactions, left polarized incoming electrons can probe CP-violation slightly better than unpolarized ones. We can see that in the tth case the CP-effect drops as the mass of the light Higgs h grows, while in the ttZ case it grows with m_h . In particular, we find that with $\sqrt{s} = 1.5$ TeV and for $m_h \sim > 2m_t$ the effect is comparable for both the tth and the ttZ cases where it reaches above 3σ for negatively polarized electrons. With a light Higgs mass in the range $100 \text{ GeV} \lesssim m_h \lesssim 160 \text{ GeV}$, the tth case is more sensitive to O_{opt} and the CP-violating effect can reach $\sim 4\sigma$ for left polarized electrons. In that light Higgs mass range, the CP-violating effect reaches slightly below 2.5σ for the ttZ case. For a c.m. energy of $\sqrt{s} = 1$ TeV and $m_h = 360$ GeV, the ttZ case is much more sensitive to O_{opt} and the effect can reach 2.2σ for left polarized electron beam. However, with that c.m. energy, the tth mode gives a better CP-odd effect in the range $100 \text{ GeV} \lesssim m_h \lesssim 160 \text{ GeV}$.

Before continuing, let us summarize the above results and add some concluding remarks. We have shown that an extremely interesting CP-odd signal may arise at tree-level in the reactions $e^+e^- \rightarrow t\bar{t}h$ and $e^+e^- \rightarrow t\bar{t}Z$. The asymmetries that were found are $\sim 15\% - 35\%$ in the tth case and $\sim 7\% - 8\%$ for the ttZ final state. These

Table 1: The statistical significance, N_{SD} , in which the CP-nonconserving effects in $e^+e^- \rightarrow t\bar{t}h$ can be detected in one year of running of a future high energy collider with either unpolarized or polarized incoming electron beam. We have used $\tan\beta = 0.5$, a yearly integrated luminosity of $\mathcal{L} = 200$ and 500 [fb]^{-1} for $\sqrt{s} = 1$ and 1.5 TeV , respectively, and an efficiency reconstruction factor of $\epsilon = 0.5$ for both energies. Recall that $j = 1(-1)$ stands for right(left) polarized electrons. Set II means $\{\alpha_1, \alpha_2, \alpha_3\} \equiv \{\pi/2, \pi/4, 0\}$.

		$e^+e^- \rightarrow t\bar{t}h$ (Model II with Set II)		
\sqrt{s} (TeV) \Downarrow	j (GeV) \Rightarrow	O_{opt}		
		$m_h = 100$	$m_h = 160$	$m_h = 360$
1	-1	2.2	2.0	1.1
	unpol	2.0	1.9	1.0
	1	1.8	1.7	0.9
1.5	-1	4.0	3.9	3.2
	unpol	3.6	3.5	2.9
	1	3.2	3.1	2.6

Table 2: The same as Table 1 but for $e^+e^- \rightarrow t\bar{t}Z$, with $\tan\beta = 0.3$. In this reaction, effects of the heavy Higgs, H , are included and N_{SD} is given for both $m_H = 750 \text{ GeV}$ (in parentheses) and $m_H = 1 \text{ TeV}$.

		$e^+e^- \rightarrow t\bar{t}Z$ (Model II with Set II)		
\sqrt{s} (TeV) \Downarrow	j (GeV) \Rightarrow	O_{opt}		
		$m_h = 100$	$m_h = 160$	$m_h = 360$
1	-1	(1.8) 1.7	(1.8) 1.8	(2.2) 2.2
	unpol	(1.6) 1.6	(1.7) 1.6	(2.0) 2.0
	1	(1.5) 1.5	(1.5) 1.5	(1.8) 1.8
1.5	-1	(2.3) 2.9	(2.4) 3.0	(2.8) 3.3
	unpol	(2.1) 2.6	(2.1) 2.7	(2.5) 3.0
	1	(1.8) 2.3	(1.8) 2.3	(2.1) 2.6

asymmetries can give rise to a $\sim 3 - 4\sigma$ CP-odd signals in a future e^+e^- collider running with c.m. energies in the range $1 \text{ TeV} \lesssim \sqrt{s} \lesssim 2 \text{ TeV}$.

Note, however, that the simple observable, O , as well as the optimal one, O_{opt} , require the identification of the t and \bar{t} and the knowledge of the transverse components of their momenta in each $t\bar{t}h$ or $t\bar{t}Z$ event. Thus, for the main top decay, $t \rightarrow bW$, the most suitable scenario is when either the t or the \bar{t} decays semi-leptonically and the other decays hadronically. Distinguishing between t and \bar{t} in the double hadronic decay case will require more effort and still remains an experimental challenge. Note, for example, that if the identification of the charge of the b-jets coming from the t and the \bar{t} is possible then the difficulty in reconstructing the transverse components of the t and \bar{t} momenta can be bypassed by using the momenta of the decay products in the processes $e^+e^- \rightarrow t\bar{t}h \rightarrow bW^+\bar{b}W^-h$ and $e^+e^- \rightarrow t\bar{t}Z \rightarrow bW^+\bar{b}W^-Z$. For example, the observable:

$$O_b = \frac{\epsilon(p_-, p_+, p_b, p_{\bar{b}})}{s^2}, \quad (29)$$

can be constructed. We have considered this observable for the reaction $e^+e^- \rightarrow t\bar{t}h \rightarrow bW^+\bar{b}W^-h$ in [3]. We found there that, close to threshold, this observable is not very effective. However at higher energies, O_b is about as sensitive as the simple triple product correlation O defined in Eq. 27 and, therefore, slightly less sensitive than O_{opt} .

Note also that for the light Higgs mass, $m_h = 100 \text{ GeV}$, the most suitable way to detect the Higgs in $e^+e^- \rightarrow t\bar{t}h \rightarrow bW^+\bar{b}W^-h$ is via $h \rightarrow b\bar{b}$ with branching ratio ~ 1 . For $m_h \gtrsim 2m_t$, and specifically with set II used above, there are two competing Higgs decays, $h \rightarrow t\bar{t}$ and $h \rightarrow W^+W^-$, depending on the value of $\tan\beta$. For example, for $\tan\beta = 0.5$, as was chosen above, one has $\text{Br}(h \rightarrow t\bar{t}) \approx 0.77$ and $\text{Br}(h \rightarrow W^+W^-) \approx 0.17$, thus, the $h \rightarrow t\bar{t}$ mode is more adequate. Of course, $h \rightarrow t\bar{t}$ will dominate more for smaller values of $\tan\beta$ and less if $\tan\beta > 0.5$. In particular, for $\tan\beta = 0.3(1)$ one has $\text{Br}(h \rightarrow t\bar{t}) \approx 0.89(0.57)$ and $\text{Br}(h \rightarrow W^+W^-) \approx 0.08(0.32)$.

As emphasized before, the final states $t\bar{t}h$ and $t\bar{t}Z$, and in particular the $t\bar{t}h$, are expected to be the center of considerable attention at a future linear collider.

Extensive studies of these reactions are expected to teach us about the details of the couplings of Higgs to the top quark. Thus, it is gratifying that the same final states promise to exhibit interesting effects of CP violation. It would be very instructive to examine the effects in other extended models. Numbers emerging from the 2HDM that was used especially with the specific value of the parameters, should be viewed as an illustrative example. The important point is that the reactions $e^+e^- \rightarrow t\bar{t}h \rightarrow bW^+\bar{b}W^-h$ and $e^+e^- \rightarrow t\bar{t}Z \rightarrow bW^+\bar{b}W^-Z$ appear to be very powerful and very clean tools for extracting valuable information on the parameters of the underlying model for CP violation.

3. $e^+e^- \rightarrow t\bar{c}\nu_e\bar{\nu}_e, t\bar{c}e^+e^-$; Cases of Tree-Level Flavor-Changing-Scalar Transitions

The reactions:

$$e^+e^- \rightarrow t\bar{c}\nu_e\bar{\nu}_e; \bar{t}c\nu_e\bar{\nu}_e, e^+e^- \rightarrow t\bar{c}e^+e^-; \bar{t}ce^+e^-, \quad (30)$$

occur via W^+W^- or ZZ fusion (see Fig. 5). The FCS transitions in those reactions gives rise to appreciable cross-sections, at the level of few fb's [6], which should be accessible to the Next generation of e^+e^- Linear Colliders.

The crucial interesting feature of the VV fusion reactions is that, being a t-channel fusion process, the corresponding cross-sections *grow* with the c.m. energy of the collider. Therefore, even if no $t\bar{c}$ events are detected at $\sqrt{s} = 500$ GeV via the previously proposed processes such as $e^+e^- \rightarrow t\bar{c}$; $t\bar{c}f\bar{f}$; $t\bar{t}c\bar{c}$ (see Atwood *et al.* and Hou *et al.* in [8]), there is still a strong motivation to look for a signature of the VV fusion processes in Eq. 30, especially at somewhat higher energies.

We note at this point that in the SM, the parton level reaction $W^+W^- \rightarrow t\bar{c}$ can also proceed at tree-level via diagram (a) in Fig. 5. However, numerically, the corresponding cross-section, $\sigma_{SM}^{\nu\bar{\nu}tc} = \sigma_{SM}(e^+e^- \rightarrow t\bar{c}\nu_e\bar{\nu}_e + \bar{t}c\nu_e\bar{\nu}_e)$, is found to be of no experimental relevance. In particular, we found that $\sigma_{SM}^{\nu\bar{\nu}tc} \approx 10^{-5} - 10^{-4}$ fb for $\sqrt{s} = 0.5 - 2$ TeV due to a severe CKM suppression [6]. We therefore neglect the SM contribution in the following.

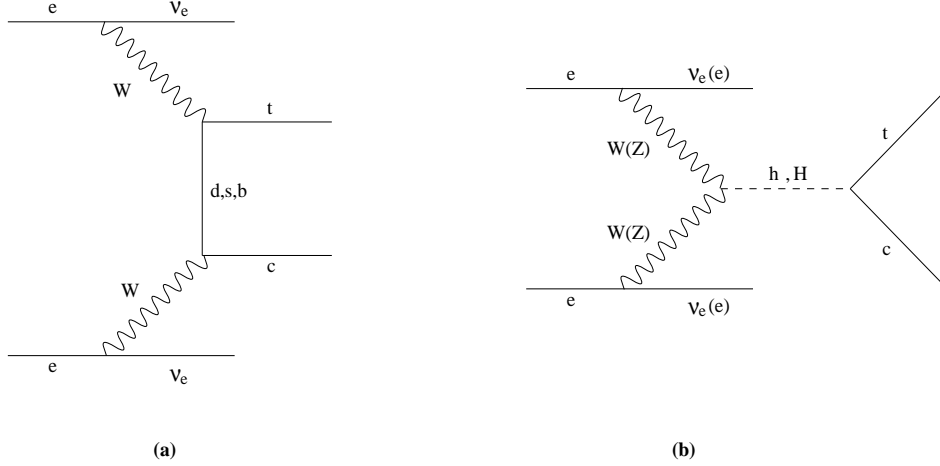


Figure 5: (a) The Standard Model diagram for $e^+e^- \rightarrow t\bar{c}\nu_e\bar{\nu}_e$; (b) Diagrams for $e^+e^- \rightarrow t\bar{c}\nu_e\bar{\nu}_e$ (e^+e^-) in Model III.

In Model III, where the $tc\mathcal{H}$ coupling of Eq. 4 are present, $VV \rightarrow t\bar{c}$ proceeds at tree-level via the \hat{s} -channel neutral Higgs exchange of diagram (b) in Fig. 5. Neglecting the SM diagram, the corresponding parton-level cross-section $\hat{\sigma}_V \equiv \hat{\sigma}(V_{\lambda_1}^1 V_{\lambda_2}^2 \rightarrow t\bar{c})$ is given by [6]:⁴

$$\hat{\sigma}_V = \frac{(\sin 2\tilde{\alpha})^2 N_c \pi \alpha^2}{4\hat{s}^2 \beta_V s_W^4} \left(\frac{m_V}{m_W}\right)^4 |\epsilon_{\lambda_1}^{V^1} \cdot \epsilon_{\lambda_2}^{V^2}|^2 |\Pi_h - \Pi_H|^2 \times m_t m_c \sqrt{a_+ a_-} (a_+ \lambda_R^2 + a_- \lambda_I^2), \quad (31)$$

where $\epsilon_{\lambda^i}^{V^i}$ ($i = 1, 2$) is the polarization vector of V^i with helicity λ^i . Also:

$$a_{\pm} = \hat{s} - (m_t \pm m_c)^2, \quad \beta_{\ell} \equiv \sqrt{1 - 4m_{\ell}^2/\hat{s}}, \quad (32)$$

and:

$$\Pi_{\mathcal{H}} = \frac{1}{(\hat{s} - m_{\mathcal{H}}^2 + im_{\mathcal{H}}\Gamma_{\mathcal{H}})}. \quad (33)$$

⁴ $V^1 = W^+, V^2 = W^-$ for W^+W^- fusion and $V^1 = V^2 = Z$ for ZZ fusion.

For definiteness, we will ignore CP violation and take $\lambda_I = 0$ and $\lambda = \lambda_R$ in Eq. 4. In calculating the full cross sections, i.e. $\sigma^{\nu\bar{\nu}tc} \equiv \sigma(e^+e^- \rightarrow t\bar{c}\nu_e\bar{\nu}_e + \bar{t}c\nu_e\bar{\nu}_e)$ and $\sigma^{eetc} \equiv \sigma(e^+e^- \rightarrow t\bar{c}e^+e^- + \bar{t}ce^+e^-)$, we used the effective vector boson approximation (EVBA) [16]. An exact calculation of $\sigma^{\nu\bar{\nu}tc}$, using $2 \rightarrow 4$ helicity amplitudes, was performed in [7], where it was found that, in the ranges where $\sigma^{\nu\bar{\nu}tc} \gtrsim 1$ fb, the difference between the EVBA and the exact calculation is about $\sim 10\%$. Note also from Eq. 31, that $\hat{\sigma}_W \rightarrow \hat{\sigma}_Z$ for $m_W \rightarrow m_Z$. The main difference between $\sigma^{\nu\bar{\nu}tc}$ and σ^{eetc} then arises from the dissimilarity between the distribution functions for W and Z bosons, and we find that $\sigma^{\nu\bar{\nu}tc} \approx 10 \times \sigma^{eetc}$ (for more details see [6]). Therefore, below we present an analysis of $\sigma^{\nu\bar{\nu}tc}$ only, keeping in mind that σ^{eetc} exhibits the same behavior though suppressed by about an order of magnitude.

As mentioned in the introduction, only two out of the three neutral Higgs particles are relevant for the present analysis. The reason is that, in the FC case also, only h and H can simultaneously have a coupling to a vector boson and a FC coupling to $t\bar{c}$. therefore there is a “GIM-like” cancellation in the scalar sector, operative also in the flavor-changing effects of Model III. In particular, the choice $\tilde{\alpha} = \pi/4$, for which the tch and tcH couplings are identical (see Eq. 4), is special in the sense that for this value the “GIM-like” cancellation mentioned above is most effective. Thus, for degenerate h and H masses and with $\tilde{\alpha} = \pi/4$, the cross-section $\sigma^{\nu\bar{\nu}tc}$ vanishes. However, for $\tilde{\alpha} \neq \pi/4$, this “GIM-like” cancellation is only partly effective and $\sigma^{\nu\bar{\nu}tc} \gtrsim 1$ fb is still possible, even with $m_H = m_h$.

In Fig. 6 we show the dependence of the scaled cross-section $\sigma^{\nu\bar{\nu}tc}/\lambda^2$ on the mass of the light Higgs m_h for four values of s and for $\tilde{\alpha} = \pi/4$.⁵ The cross-section peaks at $m_h \simeq 250$ GeV and drops as the mass of the light Higgs approaches that of the heavy Higgs due to the “GIM-like” cancellation discussed above. For c.m. energies of $\sqrt{s} \gtrsim 1$ TeV, $\sigma^{\nu\bar{\nu}tc} \gtrsim 2$ fb at the point $\tilde{\alpha} = \pi/4$, if $\lambda = 1$ and $m_h \approx 250$ GeV. It is therefore evident from Fig. 6 that at an NLC running at energies of $\sqrt{s} \gtrsim 1$ TeV and an integrated luminosity of the order of $\mathcal{L} \gtrsim 10^2$ [fb]⁻¹, Model III (with $\lambda = 1$) predicts hundreds and up to thousands of $t\bar{c}\nu_e\bar{\nu}_e$ events and several tens to hundreds of $t\bar{c}e^+e^-$ events. For example, with $\sqrt{s} = 1.5$ TeV, $\mathcal{L} = 500$ [fb]⁻¹ [1], and $m_h \approx 250$

⁵The scaled cross-section, $\sigma^{\nu\bar{\nu}tc}/\lambda^2$, has a residual mild dependence on λ through its dependence on the Higgs particles widths, $\Gamma_{\mathcal{H}}$.

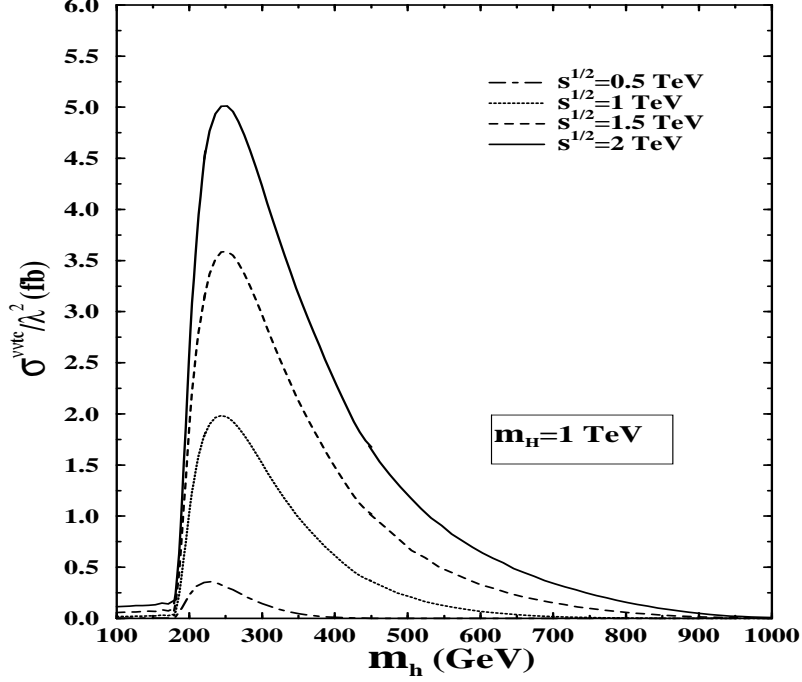


Figure 6: The cross-section $\sigma(e^+e^- \rightarrow t\bar{c}\nu_e\bar{\nu}_e + \bar{t}c\nu_e\nu_e)$ in units of λ^2 as a function of m_h for $\sqrt{s} = 0.5, 1, 1.5$ and 2 TeV. $\tilde{\alpha} = \pi/4$ and we have set $\lambda = 1$ in the width $\Gamma_{\mathcal{H}}$.

GeV, $\tilde{\alpha} = \pi/4$, $\lambda = 1$, the cross-section $\sigma^{\nu tc}(\sigma^{etc})$ would yield about 2000(200) such events. Note also that even with $m_h \approx 500$ GeV, this projected luminosity will still yield hundreds of $t\bar{c}\nu_e\bar{\nu}_e$ events and tens of $t\bar{c}e^+e^-$ events at $\sqrt{s} = 1.5$ TeV. The corresponding SM prediction yields, as mentioned above, essentially zero events.

In Fig. 7 we show the dependence of $\sigma^{\nu tc}/\lambda^2$ on $(\sin \tilde{\alpha})^2$ for $m_h = 250$ GeV, $\sqrt{s} = 1$ TeV and for two possible values of m_H , $m_H = 250$ GeV and $m_H = 1$ TeV. The same behavior is observed for any value of \sqrt{s} in the range 0.5–2 TeV. We see that in the large splitting case, i.e. $m_H = 1$ TeV, $\sigma^{\nu tc}(\pi/14 \lesssim \tilde{\alpha} \lesssim \pi/4) > \sigma^{\nu tc}(\tilde{\alpha} = \pi/4)$. Moreover, even for $(m_H - m_h) = 0$, $\sigma^{\nu tc} \gtrsim 1$ fb is still possible for $0.02 \lesssim (\sin \tilde{\alpha})^2 \lesssim 0.22$ and $0.78 \lesssim (\sin \tilde{\alpha})^2 \lesssim 0.98$. In fact, our analysis shows that, with moderate restrictions on $\tilde{\alpha}$, $\sigma^{\nu tc}$ remains well above the fb level for $\sqrt{s} \gtrsim 1$ TeV as long as one of the neutral Higgs particles (either the light one or the heavy one) is kept within $200 \text{ GeV} \lesssim m_{\mathcal{H}} \lesssim 400 \text{ GeV}$, while the mass of the other Higgs can take practically any value between 100 GeV – 1000 GeV. As was pointed out

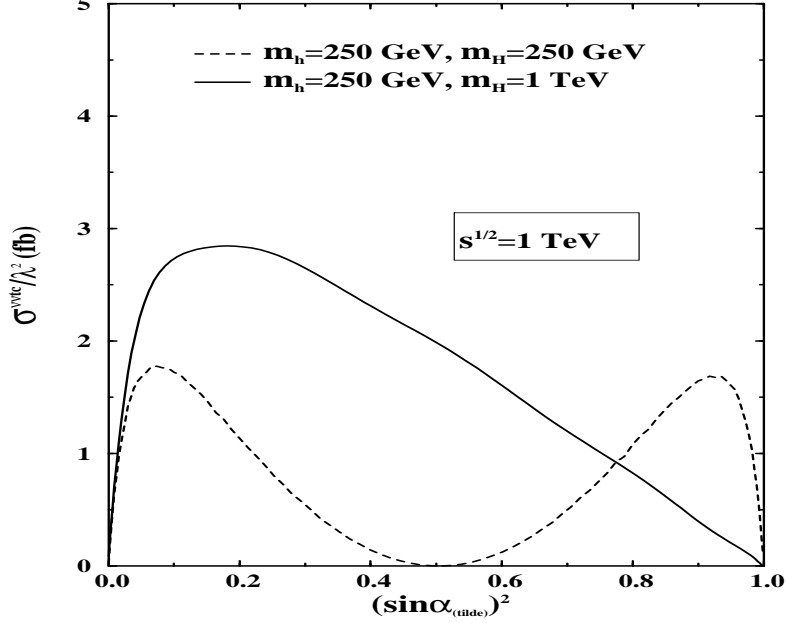


Figure 7: The cross-section $\sigma(e^+e^- \rightarrow t\bar{c}\nu_e\bar{\nu}_e + \bar{t}c\nu_e\bar{\nu}_e)$ in units of λ^2 as a function of $(\sin \tilde{\alpha})^2$ for $\sqrt{s} = 1$ TeV, $m_h = 250$ GeV and $m_H = 250, 1000$ GeV. λ as in Fig. 6.

in [7], it is interesting to note that if both m_h and m_H are of order of the weak scale and the splitting between the two masses is a few times the width of both Higgs bosons, then, with $m_h \approx 250$ GeV, $\sigma^{\nu tc}$ can reach ~ 8 fb at $\sqrt{s} = 2$ TeV. This is almost twice as large as the $m_H = 1$ TeV case. Also, Hou *et al.* have shown that the cross-section $\sigma^{\nu tc}$ depends only mildly on $\tilde{\alpha}$, when m_h and m_H are not degenerate with values of the order of few hundreds GeV. In particular, they showed that the dependence on $\tilde{\alpha}$ is only significant near the edge values $\tilde{\alpha} = 0, \pi/2$, for which the $W^+W^- \rightarrow t\bar{c}$ amplitude vanishes.

To summarize this section, it was shown that the cross-section for the reaction $e^+e^- \rightarrow t\bar{c}\nu_e\bar{\nu}_e + \bar{t}c\nu_e\bar{\nu}_e$ can reach a few fb's in a rather wide range of the Model III parameter space.⁶ Bearing the vanishingly small cross-section for this reaction in the SM (due to GIM suppression), the large cross-section predicted in Model III is

⁶Recall that the cross-section is $\propto \lambda^2$ so that even a moderate change of λ , say by a factor of three, can increase or decrease the cross-section by one order of magnitude.

especially gratifying. Therefore, this reaction may serve as a unique test of the SM and, in particular, of its GIM mechanism. From the experimental point of view, it should be emphasized that although σ^{eetc} is found to be one order of magnitude smaller than $\sigma^{\nu\bar{\nu}tc}$, the $t\bar{c}e^+e^-$ signature may be easier to detect as it does not have the missing energy associated with the two neutrinos in the $t\bar{c}\nu_e\bar{\nu}_e$ final state. Moreover, at $\sqrt{s} \gtrsim 1$ TeV, the $t\bar{c}\nu_e\bar{\nu}_e$ and $t\bar{c}e^+e^-$ signatures are to some extent unique, as other simple FC s -channel processes like $e^+e^- \rightarrow Z \rightarrow t\bar{c}$, $e^+e^- \rightarrow Z\mathcal{H} \rightarrow Zt\bar{c}$ and $e^+e^- \rightarrow A\mathcal{H} \rightarrow t\bar{t}c\bar{c}, t\bar{c}f\bar{f}$ tend to drop as $1/s$ and are therefore expected to yield much smaller production rates at an e^+e^- collider with $\sqrt{s} \gtrsim 1$ TeV.

It should be also noted that we do not anticipate serious background problems for this reaction, since it will be difficult to fake a $t\bar{c}$ event with other “normal” modes, like the $t\bar{t}$ and the W^+W^- final states, which may have higher production rates than the $t\bar{c}\nu_e\bar{\nu}_e$ mode [6]. For example, we have shown in [6], that, in Model III, the $t\bar{c}\nu_e\bar{\nu}_e$ final state may come out favorable compared to the normal $t\bar{t}\nu_e\bar{\nu}_e$, in the range where $\sigma^{\nu\bar{\nu}tc} \gtrsim 1$ fb.

Finally, in Model III, the same tree-level $VV \rightarrow t\bar{c}$ amplitude may give rise to enhanced decay and production rates of the rare three-body top decays $t \rightarrow W^+W^-c, ZZc$ and the $Zt\bar{c}$ final state through $e^+e^- \rightarrow Zt\bar{c}$ (for more detail see [6]).

4. General Concluding Remarks

To conclude this talk let us add two additional remarks:

- It is most likely that the Higgs particles, if at all present, will have been discovered by the time the NLC starts its first run. If indeed such a particle is detected with a mass of a few hundreds GeV, it will be extremely important to investigate the reactions $e^+e^- \rightarrow t\bar{t}h$, $e^+e^- \rightarrow t\bar{t}Z$, $e^+e^- \rightarrow t\bar{c}\nu_e\bar{\nu}_e$ and $e^+e^- \rightarrow t\bar{c}e^+e^-$ in the NLC, as they may serve as strong evidence for the existence of a nonminimal scalar sector with CP-violating and/or FC scalar couplings to fermions. Needless to say, such signatures of CP-violation and FCS interactions, residing in the scalar potential, will rule out the Minimal

Supersymmetric Standard Model (MSSM). In addition, since supersymmetry strongly disfavors an h heavier than ~ 150 GeV, the detection of a Higgs particle above this limit would drive the study of general extended scalar sector, not of a supersymmetric origin, and in turn, this should encourage the study of CP-nonconserving and FC effects such as the ones presented in this talk.

- It should be emphasized that the large CP-violating effects found in $e^+e^- \rightarrow t\bar{t}h$ and $e^+e^- \rightarrow t\bar{t}Z$ for Model II can be generalized to model III as well. In Model III, the CP-odd phase in the $\mathcal{H}t\bar{t}$ vertex can arise from a phase in the Yukawa couplings U_{ij}^2 and D_{ij}^2 defined in Eq. 1. With an appropriate choice of parameters, a comparable tree-level CP-odd effect may arise within Model III in $e^+e^- \rightarrow t\bar{t}h$ and $e^+e^- \rightarrow t\bar{t}Z$ (see also [4]). Thus, detection or no detection of the FC channels such as $e^+e^- \rightarrow t\bar{c}\nu_e\bar{\nu}_e$ and $e^+e^- \rightarrow t\bar{c}e^+e^-$ discussed here, along with evidence for CP-violation in the Higgs sector that could emanate in the reactions $e^+e^- \rightarrow t\bar{t}h$ and $e^+e^- \rightarrow t\bar{t}Z$ in high energy e^+e^- colliders, may well be the only way to experimentally distinguish between scalar dynamics of a Model II or a Model III origin.

References

- [1] For recent reviews on linear colliders see e.g., E. Accomando *et al.*, hep-ph/9705442; S. Kuhlman *et al.*, hep-ex/9605011; H. Murayama and M. E. Peskin, Ann. Rev. Nucl. Part. Sci. **49**, 513 (1996). See also, Proceedings of the Workshop on Physics and Experiments with Linear e^+e^- Colliders, eds. F. Harris S. Olsen, S. Pakvasa and X. Tata, World Scientific, Singapore, 1993; A. Miyamoto and Y. Fujii, *ibid*, 1996.
- [2] For a review see J. Gunion, H. Haber, G. Kane and S. Dawson, “The Higgs Hunter’s Guide”, (Addison-Wesley, New York, 1990).
- [3] S. Bar-Shalom, D. Atwood, G. Eilam, R. Mendel and A. Soni, Phys. Rev. **D53**, 1162 (1996). See also Gunion *et al.* in Refs. 12 and 13.
- [4] S. Bar-Shalom, D. Atwood and A. Soni, hep-ph/9707284, to appear in Phys. Lett. **B**.
- [5] D. Atwood and A. Soni, hep-ph/9607481.
- [6] S. Bar-Shalom, G. Eilam, A. Soni and J. Wudka, Phys. Rev. Lett **79**, 1217 (1997); Longer version in hep-ph/9708358. See also W. -S. Hou *et al.* in Ref. 7.
- [7] W. -S. Hou, G. -L. Lin and C. -Y. Ma, hep-ph/9708228.
- [8] M.J. Savage, Phys. Lett. **B266**, 135 (1991); W.S. Hou, Phys. Lett. **B296**, 179 (1992); M. Luke and M.J. Savage, Phys. Lett. **B307**, 387 (1993); L.J. Hall and S. Weinberg, Phys. Rev. **D48**, R979 (1993); D. Atwood, L. Reina and A. Soni, Phys. Rev. Lett **75**, 3800 (1995); *ibid* Phys. Rev. **D53**, 1199 (1996); W.-S. Hou and G.-L. Lin, Phys. Lett. **B379**, 261 (1996).
- [9] C.D. Froggat, R.G. Moorhouse and I.G. Knowles, Nucl. Phys. **B386** 63 (1992); W. Bernreuther, T. Schröder and T.N. Pham, Phys. Lett. **B279**, 389 (1992).
- [10] For a recent short review of Model III see: D. Atwood, L. Reina and A. Soni, Phys. Rev. **D55**, 3156 (1997).

- [11] T.P. Cheng and M. Sher, Phys. Rev. **D35**, 3484 (1987); M. Sher and Y. Yuan, Phys. Rev. **D44**, 1461 (1991).
- [12] J.F. Gunion, B. Grzadkowski and X.-G. He, Phys. Rev. Lett **77**, 5172 (1996).
- [13] J.F. Gunion and X.-G. He, hep-ph/9609453.
- [14] K. Hagiwara, H. Murayama and I. Watanabe, Nucl. Phys. **B367** 257 (1991); see also K. Fujii in the Proceedings of the 4th KEK Topical Conference on Flavor Physics (1996) and references therein.
- [15] D. Atwood and A. Soni, Phys. Rev. **D45**, 2405 (1992).
- [16] See e.g., R. Cahn and S. Dawson, Phys. Lett. **B136**, 196 (1984); **136B**, 464(E) (1984); M. Chanowitz and M.K. Gaillard, Phys. Lett. **B142**, 85 (1984); G.L. Kane, W.W. Repko and W.B. Rolnick, Phys. Lett. **B148**, 367 (1984); P.W. Johnson, F.I. Olness and W.-K. Tung, Phys. Rev. **D36**, 291 (1987).